J. Marine Sci. Appl. (2017) 16: 10-19
DOI: 10.1007/s11804-017-1392-z

A Note on the Solution of Water Wave Scattering Problem Involving Small Deformation on a Porous Channel-Bed

S. Mohapatra* **and M.R. Sarangi**

Department of Mathematics, Veer Surendra Sai University of Technology, Burla-768018, India

Abstract: The solution of water wave scattering problem involving small deformation on a porous bed in a channel, where the upper surface is bounded above by an infinitely extent rigid horizontal surface, is studied here within the framework of linearized water wave theory. In such a situation, there exists only one mode of waves propagating on the porous surface. A simplified perturbation analysis, involving a small parameter $\varepsilon(\ll 1)$, which measures the smallness of the deformation, is employed to reduce the governing Boundary Value Problem (BVP) to a simpler BVP for the first-order correction of the potential function. The first-order potential function and, hence, the first-order reflection and transmission coefficients are obtained by the method based on Fourier transform technique as well as Green's integral theorem with the introduction of appropriate Green's function. Two special examples of bottom deformation: the exponentially damped deformation and the sinusoidal ripple bed, are considered to validate the results. For the particular example of a patch of sinusoidal ripples, the resonant interaction between the bed and the upper surface of the fluid is attained in the neighborhood of a singularity, when the ripples wavenumbers of the bottom deformation become approximately twice the components of the incident field wavenumber along the positive x-direction. Also, the main advantage of the present study is that the results for the values of reflection and transmission coefficients are found to satisfy the energy-balance relation almost accurately.
Keywords: Porous bed, bottom deformation, perturbation analysis, Fourier Transform, Green's function, reflection coefficient, transmission coefficient; energy identity, water wave scattering

Article ID: 1671-9433(2017)01-0010-10

1 Introduction

In recent decades, the problems of scattering of surface water waves by an obstacle or a geometrical disturbance at the bottom of an ocean, whereas the upper surface is bounded above by either a free-surface or any floating surface(s), are important for their possible applications in the area of marine engineering, and as such these are being studied by many researchers. Various methods have introduced to study the hydrodynamic coefficients in water waves with an impermeable ocean-bed. A scattering of surface water waves by a small bottom deformation in an ocean with free surface create interesting mathematical problems drawing attention of various types for obtaining their useful solutions (Davies, 1982; Martha and Bora, 2007; Mei, 1985). The behavior of water waves over periodic beds was considered by Porter and Porter (2003) in a two-dimensional context using linear water wave theory. They developed a transfer matrix method incorporating evanescent modes for the scattering problem, which reduced the computation to that required for a single period, without compromising full linear theory. Later on, Porter and Porter (2004) investigated the three-dimensional wave scattering by an ice sheet of varying thickness floating on sea water which had undulating bed topography. They obtained a simplified form of the problem by deriving a variational principle equivalent to the governing equations of linear theory and invoking the mild-slope approximation in respect of the ice thickness and water depth variations. Wang and Meylan (2002) obtained a solution by reducing the problem to a finite domain enclosed by a boundary (including the varying part of the bed and the lower surface of the plate) on which the normal derivative of the potential is expressed as a function of the potential itself. The problem was then solved numerically using a boundary-element method. Moreover, various approaches were also developed by many researchers to deal with the interaction of water waves with floating ice plates only or the surface wave interaction by patches of small bottom undulations in an ocean with ice-cover (Chakrabarti, 2000; Linton and Chung, 2003; Mandal and Basu, 2004).

The above works focused only on the wave motion of the fluid region, where the effect of porosity of the ocean-bed was not taken into account. Studies of different types of water waves scattering problems with a permeable ocean-bed of variable depth, have gained reasonable importance due to various reasons. Tsai *et al.* (2006) investigated the wave transmission over a submerged permeable breakwater on a porous sloping seabed. Hur and Mizutani (2003) developed a numerical model to estimate the wave forces acting on a three-dimensional body on a submerged breakwater. Using the method of eigenfunction expansion technique, Maiti and Mandal (2014) analyzed the problem of water wave scattering by a thin horizontal elastic

Received date: 09-Apr-2016
Accepted date: 21-Sep-2016
Foundation item: Partially supported by a research grant from Department of Science and Technology (DST), India (No. SB/FTP/MS-003/2013).
***Corresponding author Email:** smrutiranjan.m@gmail.com

plate (both semi-infinite as well as finite) floating on an ocean of uniform finite depth in which the ocean bed is composed of porous material of a specific type. Employing the complex wavenumber in the poro-elastic model, Jeng (2001) developed the wave dispersion relation in a porous seabed. Later on, Silva *et al.* (2002) investigated the problem of water wave diffraction by a permeable ocean-bed of variable depth. Zhu (2001) considered the problem involving wave propagation within porous media on an undulating bed and solved the problem by employing Galerkin eigenfunction expansion technique. They investigated the value of the reflection coefficient numerically. Mohapatra (2014, 2015, 2016) studied the problems of water wave interaction by a small deformation on a porous bed in an ocean using Green's integral theorem with the introduction of appropriate Green's function.

In the present work, we consider a fluid flow in a channel where the upper surface is bounded above by an infinitely extent rigid horizontal surface and the bottom is bounded by a porous type surface which has a small deformation. The motion of the fluid below the porous channel bed is not analyzed here and it is assumed that the fluid motions are such that the resulting boundary condition on the porous bed as considered here holds good and depends on a known parameter P, called porosity parameter, in this analysis. In this case, time-harmonic waves of a particular porosity parameter can propagate with one wave number on the porous surface. By employing perturbation analysis, the original problem is reduced to a simpler boundary value problem for the first order correction of the potential function. The solution of this problem is then obtained by the use of Fourier transform technique and of Green's integral theorem of the potential function describing the boundary value problem. The reflection and transmission coefficients are then evaluated approximately up to the first order of ε in terms of integrals involving the shape function when a train of progressive waves propagating from negative infinity is normally incident on the porous channel bed having a small deformation. We present two special forms of bottom deformation, that is, the exponentially damped deformation and a patch of sinusoidal ripples, and the first-order refection and transmission coefficients are depicted graphically for various values of the different parameters.

2 Formulation of the physical problem

We consider the irrotational motion of an inviscid incompressible fluid of relatively small amplitude under the action of gravity, having a porous bottom surface, whereas the upper surface of the fluid is covered by an infinitely extent rigid horizontal surface. The fluid is of infinite horizontal extent in x-direction while the depth is along y-direction which is considered vertically downwards with $y=0$ as the mean position of the rigid surface and $y=h$ as the bottom surface. We further assume that the motion is time harmonic with angular frequency ω. Here, the bed has a small deformation, which is described by $y=h+\varepsilon c(x)$, where $c(x)$ is a differentiable function and the non-dimensional number $\varepsilon(=1)$ a measure of the smallness of the deformation. Under the assumptions of the linear water wave theory, the complex-valued potential function $\Phi(x,y,t)$ in the fluid of density ρ can be written as

$$\Phi(x,y,t)=\operatorname{Re}\left[\phi(x,y)\mathrm{e}^{-\mathrm{i}\omega t}\right],\ -\infty<x<\infty,\ 0\le y\le h+\varepsilon c(x) \tag{1}$$

where the function $\phi(x,y)$ satisfies the Laplace's equation:

$$\nabla^2_{x,y}\phi=0,\ -\infty<x<\infty,\ 0\le y\le h+\varepsilon c(x), \tag{2}$$

where $\nabla^2_{x,y}=\partial^2/\partial x^2+\partial^2/\partial y^2$. The linearized boundary conditions near the top surface and at the bottom surface being given by:

$$\phi_y=0 \quad \text{on} \quad -\infty<x<\infty, y=0 \tag{3}$$

$$\phi_n-P\phi=0, \ \text{on} \quad -\infty<x<\infty, y=h+\varepsilon c(x) \tag{4}$$

where $\partial/\partial n$ the derivative normal to the bottom at a point (x,y) and P is the porous effect parameter on the porous bed. The time dependence of $\mathrm{e}^{-\mathrm{i}\omega t}$ has been suppressed.

The porous boundary condition used here is the same as that used earlier by Chwang (1983), Sahoo *et al.* (2000), Martha and Bora (2007). Bottom condition (4) was proposed by Darcy, in connection with porous bed, like a sand bed or any other loose bed (non-rigid) through which fluid may pour. The porous bed assumption induces a boundary condition of the impedance type involving a linear combination of the potential function (for the case of irrotational flow) and its normal derivative on the boundary, as used in the present paper and in the work of previous researchers.

Within this framework in the fluid, a train of two-dimensional normally incident progressive wave along the positive x-axis takes the form (up to an arbitrary multiplicative constant):

$$\phi_0(x,y)=\mathrm{e}^{\mathrm{i}p_0x}f(p_0,y),\ -\infty<x<\infty, 0\le y\le h \tag{5}$$

where

$$f(p_0,y)=\frac{\cosh p_0(h-y)-(P/p_0)\sinh p_0(h-y)}{\cosh p_0h-(P/p_0)\sinh p_0h} \tag{6}$$

with $\cosh p_0h-(P/p_0)\sinh p_0h\neq 0$ and the non-zero positive real number p_0 satisfies the dispersion relation

$$\mathfrak{F}(\upsilon)\equiv\upsilon\sinh\upsilon h-P\cosh\upsilon h=0 \tag{7}$$

In the above dispersion equation, there are two non-zero real roots $\pm p_0$, that indicate the propagating modes; and a countable infinity of purely imaginary roots $\pm \mathrm{i}p_n(n=1,2,...)$ that relate to a set of evanescent modes, where p_n's are real and positive satisfying the following equation

$$p_n\sin p_nh+P\cos p_nh=0 \tag{8}$$

It may be noted that the positive roots of the dispersion equation (7), being wavenumbers of the waves travelling in the positive direction, while the negative roots being wavenumbers of the waves travelling in the negative direction.

Assuming, for small bottom deformation, ε to be very small and neglecting the second order terms, the boundary condition (4) on the bottom surface $y = h + \varepsilon c(x)$ can be expressed in an appropriate form as

$$\phi_y - \varepsilon \frac{\mathrm{d}}{\mathrm{d}x}\left[c(x)\phi_x\right] - P\left[\phi + \varepsilon c(x)\phi_y\right] + O\left(\varepsilon^2\right) = 0 \quad \text{on } y = h \tag{9}$$

Since the wave train is partially reflected and partially transmitted over the bottom deformation, the far-field behavior of $\phi(x,y)$ is given by

$$\phi(x,y) \sim \left(A^{\pm}\mathrm{e}^{\pm\mathrm{i}p_0 x} + B^{\pm}\mathrm{e}^{\mp\mathrm{i}p_0 x}\right) f\left(p_0, y\right), \text{ as } x \to \pm\infty \tag{10}$$

A convenient short notation for (10) is,

$$\phi \sim \left(A^-, B^-; A^+, B^+\right) \tag{11}$$

where $A^{\pm}, B^{\pm}$ denote the amplitudes as $x \to \pm\infty$ of the outgoing and incoming waves set up at either infinities. For this diffraction problem, the far-field form of potential function ϕ is given by

$$\phi \sim \left(R, 1; T, 0\right) \tag{12}$$

where the unknown complex constants R and T are related to the reflection and transmission coefficients, respectively, and are to be determined. Here, the perturbation method can be employed to obtain these coefficients up to first order. By using the perturbation technique, the entire fluid region $0 \le y \le h + \varepsilon c(x)$, $-\infty < x < \infty$, is reduced to the uniform finite strip $0 \le y \le h$, $-\infty < x < \infty$, in the following mathematical analysis.

3 Solution of the problem

In this section, we will consider the scattering problem for a normally incident wave propagates over a porous bed which has a small deformation, whereas the top surface of the fluid is bounded by a rigid surface. Using perturbation analysis, the corresponding problem will reduce up to first-order to a Boundary Value Problem (BVP) which will be solved by Fourier transform technique and Green's function technique.

Consider a train of progressive waves to be normally incident on the bottom deformation. If there is no bottom deformation, then the normally incident waves will propagate without any hindrance and there will be only transmission. This, along with the appropriate form of the boundary condition (9), suggest that $\phi(x,y)$, R and T which were introduced in the last section, can be expressed in terms of the small parameter ε as:

$$\left.\begin{aligned} &\phi(x,y) = \phi_0(x,y) + \varepsilon\phi_1(x,y) + O\left(\varepsilon^2\right), \\ &R = \varepsilon R_1 + O\left(\varepsilon^2\right), \\ &T = 1 + \varepsilon T_1 + O\left(\varepsilon^2\right), \end{aligned}\right\} \tag{13}$$

where $\phi_0(x,y)$ is given by Eq. (5). It must be noted that such a perturbation expansion ceases to be valid at Bragg resonance when the reflection coefficient becomes much larger than the deformation parameter ε, as pointed out by Mei (1985). Also, this theory is valid only for infinitesimal reflection and away from resonance. For large reflection, the perturbation series, as defined in Eq. (13), needs to be refined so that it can deal with the resonant case, which is reported in Mei (1985).

Using Eq. (13) in Eq. (2) and the boundary conditions (3), (9), (12) and then comparing the first order terms of ε on both sides of the equations, we find a BVP for the first order potential $\phi_1(x,y)$ which satisfies

$$\nabla^2_{x,y}\phi_1 = 0, \ -\infty < x < \infty, 0 \le y \le h \tag{14}$$

$$\phi_{1y} = 0 \quad \text{on} \quad -\infty < x < \infty, y = 0 \tag{15}$$

$$\phi_{1y} - P\phi_1 = \frac{\mathrm{i}p_0 \dfrac{\mathrm{d}}{\mathrm{d}x}\left[c(x)\mathrm{e}^{\mathrm{i}p_0 x}\right] + P^2 c(x)\mathrm{e}^{\mathrm{i}p_0 x}}{\cosh p_0 h - (P/p_0)\sinh p_0 h} \equiv U(x, p_0) \tag{16}$$
$$\text{on} \quad -\infty < x < \infty, \ y = h$$

and $\phi_1(x,y)$ has the far-field behaviour as

$$\phi_1 \sim \left(R_1, 0; T_1, 0\right) \tag{17}$$

3.1 Introduction of Fourier transforms

To solve the above BVP, we now assume that the potential function $\phi_1(x,y)$ of the fluid is such that the Fourier transform with respect to x, denoted by $\overline{\phi_1}(\xi,y)$ exists and is defined by

$$\overline{\phi_1}(\xi,y) = \int_{-\infty}^{\infty} \phi_1(x,y)\,\mathrm{e}^{-\mathrm{i}\xi x}\,\mathrm{d}x \tag{18}$$

Applying the Fourier transform to equations (14)-(16), we get the following BVP for $\overline{\phi_1}(\xi,y)$ as

$$\overline{\phi}_{1yy} - \xi^2\overline{\phi_1} = 0 \quad \text{in } 0 \le y \le h \tag{19}$$

$$\overline{\phi}_{1y} = 0 \quad \text{on } y = 0 \tag{20}$$

$$\overline{\phi}_{1y} - P\overline{\phi_1} = \overline{U}(\xi, p_0) \quad \text{on } y = h \tag{21}$$

where $\overline{\phi}_{1yy}$, $\overline{\phi}_{1y}$, $\overline{\phi_1}$ and $\overline{U}(\xi,p_0)$ are the Fourier transforms of ϕ_{1yy}, ϕ_{1y}, ϕ_1 and $U(x,p_0)$, respectively. The solution $\overline{\phi_1}(\xi,y)$ of the above BVP is obtained as

$$\overline{\phi_1}(\xi,y) = \left[\frac{\overline{U}(\xi,p_0)}{\mathfrak{F}(\xi)}\right]\cosh\xi y \tag{22}$$

where

$$\overline{U}(\xi,p_0) = \frac{\left(P^2 - p_0\xi\right)}{\cosh p_0 h - (P/p_0)\sinh p_0 h}\int_{-\infty}^{\infty} c(x)\mathrm{e}^{\mathrm{i}(p_0-\xi)x}\,\mathrm{d}x \tag{23}$$

$$\mathcal{F}(\xi) \equiv \xi \sinh \xi h - P \cosh \xi h \tag{24}$$

Now we can write the inverse Fourier transform as

$$\phi_1(x,y) = \frac{1}{2\pi} \int_{-\infty}^{\infty} \overline{\phi_1}(\xi,y)\, e^{i\xi x}\, d\xi \tag{25}$$

Using the inverse Fourier transform to the Eq. (22), the solution for the potential function $\phi_1(x,y)$ of the fluid is obtained as follows:

$$\phi_1(x,y) = \frac{1}{2\pi} \int_0^{\infty} \left[\frac{\overline{U}(\xi,p_0)\, e^{i\xi x} + \overline{U}(-\xi,p_0)\, e^{-i\xi x}}{\mathcal{F}(\xi)} \right] \cosh \xi y\, d\xi \tag{26}$$

Since $\mathcal{F}(\xi)$ has one non-zero positive root at $\xi = p_0$ on the positive real axis of ξ, so the above integral contains a pole at $\xi = p_0$. Therefore, we make the path for the integral indented below the pole at $\xi = p_0$.

Now the first-order reflection and transmission coefficients R_1 and T_1, respectively, can be obtained by comparing the behaviors of $\phi_1(x,y)$ as $x \to \mp\infty$ obtained from (26) using (17). To find the behavior as $x \to \infty$, we rotate the contour in the integral involving $e^{i\xi x}$ in the first quadrant by an angle $\beta(0 < \beta < \pi/2)$ and the contour in the integral involving $e^{-i\xi x}$ in the fourth quadrant by the same angle β. As $x \to \infty$, the integral involving $e^{i\xi x}$ will only contribute a term arising from the residue at $\xi = p_0$, while there will be no contribution from the integral involving $e^{-i\xi x}$. Thus, as $x \to \infty$, the resultant integral of (26) is

$$\phi_1(x,y) = \frac{i\overline{U}(p_0,p_0)\, e^{ip_0 x} \cosh p_0 y}{\mathcal{F}'(p_0)} = \frac{i\overline{U}(p_0,p_0)\, e^{ip_0 x}[\cosh p_0(h-y) - (P/p_0)\sinh p_0(h-y)]}{\mathcal{F}'(p_0)[\cosh p_0 h - (P/p_0)\sinh p_0 h]} \tag{27}$$

where $\mathcal{F}'$ denotes the derivative of $\mathcal{F}$ with respect to ξ. Then comparing the above resultant integral value with Eq. (17), we obtain the value of T_1 as

$$T_1 = \frac{i(P^2 - p_0^2)}{\mathcal{F}'(p_0)[\cosh p_0 h - (P/p_0)\sinh p_0 h]} \int_{-\infty}^{\infty} c(x)\, dx \tag{28}$$

Similarly, to find the first-order refection coefficient R_1, we let $x \to -\infty$, in Eq. (26). To find the behavior as $x \to -\infty$, we rotate the contour in the integral involving $e^{-i\xi x}$ in the first quadrant and the contour in the integral involving $e^{i\xi x}$ in the fourth quadrant. As $x \to -\infty$, the integral involving $e^{-i\xi x}$ will only contribute a term arising from the residue at $\xi = p_0$, while there will be no contribution from the integral involving $e^{i\xi x}$. Then comparing the resultant integral value with Eq. (17), we obtain the value of R_1 as follows:

$$R_1 = \frac{i(P^2 + p_0^2)}{\mathcal{F}'(p_0)[\cosh p_0 h - (P/p_0)\sinh p_0 h]} \int_{-\infty}^{\infty} c(x)\, e^{2ip_0 x}\, dx \tag{29}$$

Therefore, the first-order reflection and transmission coefficients can be evaluated, once the shape function $c(x)$ of the bottom deformation on the porous bed is known.

3.2 Green's function technique

To solve the boundary value problem for ϕ_1 given by Eqs. (14) − (17), we need a two-dimensional source potential (in terms of Green's function) for Laplace's equation due to a source submerged in the fluid. Then Green's integral theorem will be employed and the first-order coefficients R_1 and T_1 will be obtained in terms of integrals involving the shape function $c(x)$.

Suppose the source is submerged in the fluid. Then, for $0 < \eta < h$, the source potential in terms of Green's function $G(x,y;\xi,\eta)$ satisfies the following boundary value problem

$$\nabla^2_{x,y} G = 0 \quad \text{in } 0 < y < h, \text{ except at } (\xi,\eta) \tag{30}$$

$$G_y = 0 \quad \text{on } y = 0 \tag{31}$$

$$G_y - PG = 0 \quad \text{on } y = h \tag{32}$$

$$G \sim \ln r \quad \text{as } r = \sqrt{(x-\xi)^2 + (y-\eta)^2} \to 0 \tag{33}$$

and G represents outgoing waves as $|x-\xi| \to \infty$. Now, we try to solve the boundary value problem defined by Eqs. (30)-(33) in the form $G(x,y;\xi,\eta)$, where

$$G(x,y;\xi,\eta) = \ln\frac{r}{r'} + \int_0^{\infty} [A(k)\cosh k(h-y) + B(k)\sinh ky] \cos k(x-\xi)\, dk \tag{34}$$

and $r' = \sqrt{(x-\xi)^2 + (y+\eta)^2}$. With the help of the boundary conditions at the top surface and at the bottom surface, we find $A(k)$ and $B(k)$ as

$$A(k) = \frac{2[k\cosh k(h-\eta) - P\sinh k(h-\eta)]}{k\cosh kh\, \mathcal{F}(k)} \tag{35}$$

$$B(k) = \frac{2e^{-kh}(1 + P/k)\sinh k\eta + PA}{k\cosh kh - P\sinh kh} \tag{36}$$

where $\mathcal{F}$ is same as in Eq. (7). It may be noted that $\mathcal{F}$ has one simple non-zero root at $k = p_0$. Since $k = 0$ and $\cosh kh - (P/k)\sinh kh = 0$ will indicate that there is no wave in the region, hence the terms k and $\cosh kh - (P/k)\sinh kh$ can never be zero. So the integrand in Eq. (34) have one simple pole at $k = p_0$ which will be from $\mathcal{F}(k)$ only. Since the source potential G behaves like outgoing waves as $|x-\xi| \to \infty$, so the path of integration is indented to pass beneath the simple pole at $k = p_0$. Solving (34) by using (35) and (36), we obtain the solution $G(x,y;\xi,\eta)$ as:

$$G=\frac{2\pi\mathrm{i}\left[\cosh p_0(h-\eta)-\frac{P}{p_0}\sinh p_0(h-\eta)\right]\mathrm{e}^{\mathrm{i}p_0|x-\xi|}}{\cosh p_0h\left[\cosh p_0h-\frac{P}{p_0}\sinh p_0h\right]\mathfrak{F}'(p_0)}\times$$
$$\left[\left(\cosh p_0h-\frac{P}{p_0}\sinh p_0h\right)\cosh p_0(h-y)+\frac{P}{p_0}\sinh p_0y\right]+$$
$$2\pi\sum_{n=1}^{\infty}\frac{\left[\cos p_n(h-\eta)-\frac{P}{p_n}\sin p_n(h-\eta)\right]\mathrm{e}^{-p_n|x-\xi|}}{\cos p_nh\left[\cos p_nh-\frac{P}{p_n}\sin p_nh\right]\mathfrak{F}_1(p_n)}\times$$
$$\left[\left(\cos p_nh-\frac{P}{p_n}\sin p_nh\right)\cos p_n(h-y)+\frac{P}{p_n}\sin p_ny\right] \tag{37}$$

where $\mathfrak{F}_1(p_n)=(1-Ph)\sin p_nh+p_nh\cos p_nh$. Since the source potential in terms of Green's function $G(x,y;\xi,\eta)$ behaves like outgoing waves at infinity, so taking $|x-\xi|\to\infty$, we obtain the solution $G(x,y;\xi,\eta)$ as:

$$G=\frac{2\pi\mathrm{i}\left[\cosh p_0(h-\eta)-\frac{P}{p_0}\sinh p_0(h-\eta)\right]\mathrm{e}^{\mathrm{i}p_0|x-\xi|}}{\cosh p_0h\left[\cosh p_0h-\frac{P}{p_0}\sinh p_0h\right]\mathfrak{F}'(p_0)}\times$$
$$\left[\left(\cosh p_0h-\frac{P}{p_0}\sinh p_0h\right)\cosh p_0(h-y)+\frac{P}{p_0}\sinh p_0y\right] \tag{38}$$

To calculate the value of $\phi_1(\xi,\eta)$, we apply the Green's integral theorem to $\phi_1(x,y)$ and $G(x,y;\xi,\eta)$ in the form

$$\int_C(\phi_1G_n-G\phi_{1n})\mathrm{d}s=0 \tag{39}$$

where C is a closed contour in the xy-plane consisting of the lines $y=0,-X\le x\le X$; $y=h,-X\le x\le X$; $x=\pm X, 0\le y\le h$ and a small circle $(x-\xi)^2+(y-\eta)^2=\gamma^2$, and ultimately let $X\to\infty$ and $\gamma\to 0$. Finally the resultant integral equation (39) will give the determination of the solution ϕ_1 of the boundary value problem as given by

$$\phi_1(\xi,\eta)=\frac{1}{2\pi P}\int_{-\infty}^{\infty}G_y(x,h;\xi,\eta)\,U(x,p_0)\,\mathrm{d}x \tag{40}$$

where $G_y=\partial G/\partial y$.

The first order transmission and reflection coefficients T_1 and R_1, respectively, are now obtained by letting $\xi\to\pm\infty$, in Eq. (40) and comparing with the far-field condition given in Eq. (17) by replacing (x,y) with (ξ,η).

As $\xi\to\infty$, we note from Eqs. (17) and (38), respectively, that

$$\phi_1(\xi,\eta)=T_1\phi_0(\xi,\eta) \tag{41}$$

$$G_y(x,h;\xi,\eta)=$$
$$2\pi\mathrm{i}\times\frac{\left[\cosh p_0(h-\eta)-\frac{P}{p_0}\sinh p_0(h-\eta)\right]\mathrm{e}^{-\mathrm{i}p_0(x-\xi)}}{\left[\cosh p_0h-\frac{P}{p_0}\sinh p_0h\right]\mathfrak{F}'(p_0)} \tag{42}$$

Substituting Eqs. (41) and (42) in Eq. (40), we obtain the value of T_1 as

$$T_1=\frac{\mathrm{i}}{\mathfrak{F}'(p_0)}\int_{-\infty}^{\infty}\mathrm{e}^{-\mathrm{i}p_0x}\,U(x,p_0)\,\mathrm{d}x=$$
$$\frac{\mathrm{i}\left(P^2-p_0^{\,2}\right)}{\mathfrak{F}'(p_0)\left[\cosh p_0h-\frac{P}{p_0}\sinh p_0h\right]}\int_{-\infty}^{\infty}c(x)\,\mathrm{d}x \tag{43}$$

Similarly, as $\xi\to-\infty$, we also note from Eqs. (17) and (38), respectively, that

$$\phi_1(\xi,\eta)=R_1\phi_0(-\xi,\eta) \tag{44}$$

$$G_y(x,h;\xi,\eta)=$$
$$2\pi\mathrm{i}\times\frac{\left[\cosh p_0(h-\eta)-\frac{P}{p_0}\sinh p_0(h-\eta)\right]\mathrm{e}^{\mathrm{i}p_0(x-\xi)}}{\left[\cosh p_0h-\frac{P}{p_0}\sinh p_0h\right]\mathfrak{F}'(p_0)} \tag{45}$$

Substituting Eqs. (44) and (45) in Eq. (40), we obtain the value of R_1 as

$$R_1=\frac{\mathrm{i}}{\mathfrak{F}'(p_0)}\int_{-\infty}^{\infty}\mathrm{e}^{\mathrm{i}p_0x}\,U(x,p_0)\,\mathrm{d}x=$$
$$\frac{\mathrm{i}\left(P^2+p_0^{\,2}\right)}{\mathfrak{F}'(p_0)\left[\cosh p_0h-\frac{P}{p_0}\sinh p_0h\right]}\int_{-\infty}^{\infty}\mathrm{e}^{2\mathrm{i}p_0x}c(x)\,\mathrm{d}x \tag{46}$$

Therefore, the first-order transmission and reflection coefficients can be evaluated from Eqs. (43) and (46), once the shape function $c(x)$ of the bottom deformation is known.

It may be noted here that the representations of first-order transmission and reflection coefficients, given by (43) and (46), are coinciding with the representations obtained in Fourier transform technique given by (28) and (29), respectively.

4 Energy balance relation

In the theoretical study of scattering of water waves, a special relation known as energy balance relation or energy identity which plays a very important role in checking the method of solution of such mixed boundary value problem. The energy identity relates the refection as well as transmission coefficients associated with the scattering problem and, in cases when one has to rely only on the numerical results for these important physical quantities, such identity supports the validity of the analytical as well as numerical techniques employed to solve the boundary value problem under consideration. In this section, the energy identity or energy balance relation is derived from the appropriate use of Green's integral theorem involving the complex velocity potential and its complex conjugate.

To obtain the energy identity, we use the Green's integral theorem, as given by

$$\int_{C^*}\left(\phi\bar{\phi}_n-\bar{\phi}\,\phi_n\right)\mathrm{d}s=0 \tag{47}$$

where C^* denotes the closed boundary of the fluid region, $\bar{\phi}$ is the complex conjugate of ϕ which satisfies Eqs. (2)-(4) and the far-field condition

$$\bar{\phi}\sim\left(1,\bar{R};\,0,\bar{T}\right) \tag{48}$$

and $\partial/\partial n$ represents the outward normal derivative to the boundary C^*.

We now choose C^* to be the closed boundary of the fluid region bounded by

$y=0,|x|\le X;\ 0\le y\le h, x=X;\ y=h,|x|\le X$

and $0\le y\le h,\ x=-X$

and ultimately letting $X\to\infty$.

Now using the line integrals, Eq. (47) can be written as

$$\left(\int_{y=h,|x|\le X}-\int_{0\le y\le h,x=X}-\int_{y=0,|x|\le X}+\int_{0\le y\le h,x=-X}\right)\left(\phi\bar{\phi}_n-\bar{\phi}\,\phi_n\right)\mathrm{d}s=0 \tag{49}$$

Using the top surface condition near the rigid surface and the bottom condition at the porous bed, the first and third integrals in (43) become identically zero for any value of x.

Using the far-field behaviours for ϕ and $\bar{\phi}$ as $x\to\infty$ given in equations (12) and (48), respectively, the second integral in Eq. (49) becomes

$$\int_{0\le y\le h,x=X}\left(\phi\bar{\phi}_x-\bar{\phi}\,\phi_x\right)\mathrm{d}y=-2ip_0|T|^2\int_0^h f^2(p_0,y)\,\mathrm{d}y \tag{50}$$

Similarly, using the asymptotic behaviours for ϕ and $\bar{\phi}$ as $x\to-\infty$ given in equations (12) and (48), respectively, the fourth integral in Eq. (49) becomes

$$\int_{0\le y\le h,x=-X}\left(\phi\bar{\phi}_x-\bar{\phi}\,\phi_x\right)\mathrm{d}y=2ip_0\left(|R|^2-1\right)\int_0^h f^2(p_0,y)\,\mathrm{d}y \tag{51}$$

Now substituting all the corresponding integral values in equation (49), we obtain a relation in terms of reflection and transmission coefficients as

$$|R|^2+|T|^2=1 \tag{52}$$

Eq. (52) is called as energy balance relation or energy identity.

5 Particular forms of bottom profile

In this section, we present two different forms of shape function for the bottom deformation: the exponentially damped deformation and the sinusoidal ripple bed, to validate the analytical results.

5.1 Example-I

Consider the shape function of the bottom deformation is given by

$$c(x)=a_0\,\mathrm{e}^{-b|x|},\ (b>0)\qquad -\infty<x<\infty \tag{53}$$

This shape function corresponds to an exponentially damped deformation on a porous channel bed. In this example, the top of the elevation lies at $(0,a_0)$ and it decreases exponentially on either side. In order to calculate the transmission coefficient T_1, substituting the value of $c(x)$ from (53) into (43), we obtain

$$T_1=\frac{2i\left(P^2-p_0^{\,2}\right)a_0}{\mathfrak{F}'(p_0)\,b\left[\cosh p_0h-\dfrac{P}{p_0}\sinh p_0h\right]} \tag{54}$$

In a similar way, we can calculate R_1 by substituting $c(x)$ from (53) into (46),

$$R_1=\frac{2i\left(P^2+p_0^{\,2}\right)a_0b}{\mathfrak{F}'(p_0)\left(4p_0^{\,2}+b^2\right)\left[\cosh p_0h-\dfrac{P}{p_0}\sinh p_0h\right]}. \tag{55}$$

5.2 Example-II

Here, we proceed to examine the effects of reflection and transmission for a special sinusoidal form of the shape function $c(x)$ in the form:

$$c(x)=\begin{cases}a\sin(lx+\vartheta), & -(n\pi+\vartheta)/l\le x\le(m\pi-\vartheta)/l\\ 0 & \text{otherwise}\end{cases} \tag{56}$$

where m and n are positive integers and ϑ is the phase angle of the bottom deformation on the porous channel bed. This patch of sinusoidal ripples on the surface of a porous bed having the wavenumber l with amplitude a consists of $(m+n)/2$ ripples. The corresponding first-order transmission and reflection coefficients T_1 and R_1, respectively, are obtained as follows:

$$T_1=\frac{ia\left(P^2-p_0^2\right)\left[(-1)^n-(-1)^m\right]}{\mathfrak{F}'(p_0)\,l\left[\cosh p_0h-\dfrac{P}{p_0}\sinh p_0h\right]} \tag{57}$$

$$R_1=\frac{ial\left(P^2+p_0^{\,2}\right)\left[(-1)^n\,\mathrm{e}^{-2ip_0(n\pi+\vartheta)/l}-(-1)^m\,\mathrm{e}^{2ip_0(m\pi-\vartheta)/l}\right]}{\mathfrak{F}'(p_0)\left(l^2-4p_0^{\,2}\right)\left[\cosh p_0h-\dfrac{P}{p_0}\sinh p_0h\right]}. \tag{58}$$

It is clear from (57) that when the total number of ripples in the patch of sinusoidal ripples of the porous channel-bed is a positive integer (i.e., both m and n are even or odd), T_1 vanishes identically.

In Eq. (58), when the sinusoidal ripples wave number is approximately twice the surface wave number (*i.e.,* $2p_0\approx l$, the theory points towards the possibility of a resonant interaction taking place between the bed and the surface waves. Hence, near resonance, *i.e.*, $2p_0 \approx l$, the limiting value of the reflection coefficient assumes the value

$$R_1 = -\frac{\pi a\left(m+n\right)\left(P^2+p_0^{\ 2}\right)\mathrm{e}^{-\mathrm{i}\vartheta}}{2l\mathfrak{F}'\left(p_0\right)\left[\cosh p_0 h - \dfrac{P}{p_0}\sinh p_0 h\right]} \tag{59}$$

Note that when $2p_0$ approaches l and the number of ripples in the patch of deformation on the porous bed $(m+n)/2$ becomes large, the reflection coefficient becomes unbounded contrary to our assumption that R_1 is a small quantity, being the first-order correction of the infinitesimal reflection. Consequently, we consider only the cases excluding these two conditions in order to avoid the contradiction arising out of resonant cases. Thus, near resonance, the reflection coefficient R_1 becomes a constant multiple of the total number of ripples in the patch. Hence, the reflection coefficient R_1 increases linearly with m and n. Although the theory breaks down when $l = 2p_0$, a large amount of reflection of the incident wave energy by this special form of bed surface will be generated in the neighborhood of the singularity at $l = 2p_0$.

6 Numerical results

Here, we study the behaviors of the non-dimensionalized first-order reflection and transmission coefficients related to two particular forms of bottom profile on the channel bed: the exponentially damped deformation and the sinusoidal ripple bed, where an incident surface wave of wavenumber $p_0 h$ propagating on the porous surface. In Figs. 1 and 2, which correspond to the exponentially damped deformation on the porous channel-bed, the numerical results for $|R_1|$ and $|T_1|$, calculated from (55) and (54), respectively, are plotted against *Ph* for different heights of the hump on the bottom deformation. Here, we fixed the non-dimensionalized parameter *bh* as 0.3. From these figures, it is evident that the values of both $|R_1|$ and $|T_1|$ increase against the porosity parameters when the height of the hump of the bottom deformation increases. This means that when an incident wave propagates over a small bottom deformation on a porous bed, a substantial amount of reflected and transmitted energy can be produced. Moreover, the first-order correction to the reflected and transmitted energies are sensitive to the changes in the heights of the hump on the bottom deformation on the porous channel-bed. Here, the reflected energy is comparatively much smaller than the transmitted energy. It is also observed that the non-oscillating nature of first-order correction to the reflected and transmitted energy as functions of the porosity parameters *Ph* of the channel-bed.

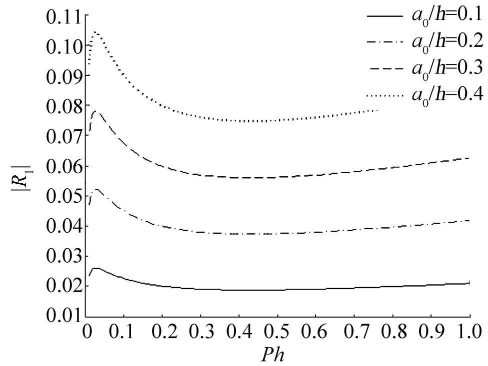

Fig. 1 Variation of $|R_1|$ plotted for various heights of exponentially damped bed

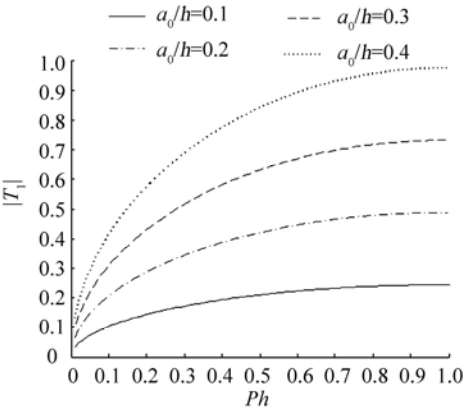

Fig. 2 Variation of $|T_1|$ plotted for various heights of exponentially damped bed

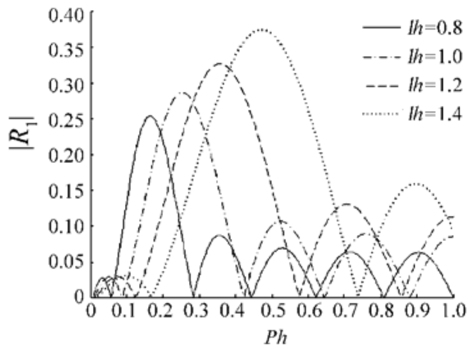

Fig. 3 Variation of $|R_1|$ plotted for various ripple wave numbers of sinusoidal bed.

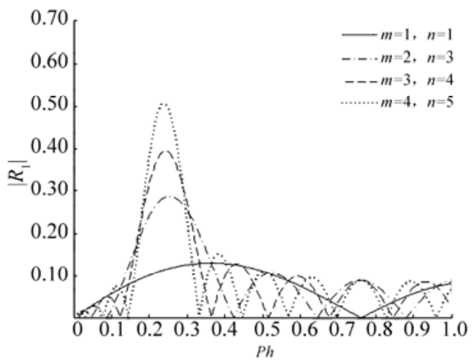

Fig. 4 Variation of $|R_1|$ plotted for various number of ripples in the patch of sinusoidal bed.

In Figs. 3 and 4, the numerical computation and graphical presentation are shown for $|R_1|$, related to a sinusoidal form of the bottom surface on the porous channel bed mentioned in Example-II. We consider the numerical computation for $|R_1|$, which is calculated from (58), due to a train of incident surface waves of wavenumber p_0h propagating on the porous surface and a ripple bed with wave number l having $(m+n)/2$ number of ripple wavelengths in the patch of the bottom deformation on a porous channel bed. In such situation, we consider the ratio of the amplitude of the ripples and the depth of the fluid (a/h) as 0.1 and the phase angle of bottom deformation $\vartheta = 0$. In Fig. 3, the different curves are plotted against *Ph* correspond to the first-order reflection coefficient $|R_1|$ for different ripple wave numbers in the patch of the deformation on the porous channel bed, while we fixed $m=2$ and $n=3$. This is most evident in the curves that the peak value of the reflection coefficient increases as the ripple wave number increases. This shows that the first-order correction to the reflected energy is somewhat sensitive to the changes in the ripple wave numbers in the patch of bottom deformation on the porous bed. Computations show that the peak values of the first-order reflection coefficient $|R_1|$ corresponding to the ripple wave numbers $lh = 0.8, 1, 1.2$ and 1.4 are attained at p_0h=0.410985, $0.521813, 0.638464$ and 0.744114, respectively. It has been observed from these results that the peak values of the reflection coefficient are attained at different values of *Ph*. The reason is, the peak value of the reflection coefficient is attained only when the ripple wave number *lh* of the bottom deformation becomes approximately twice as large as the surface wave number p_0h. It is observed from this figure that as the ripple wave numbers increase the reflection coefficient $|R_1|$ becomes smaller than those for the bigger ripple wave numbers. That means when an incident wave propagates over a small bottom deformation on the porous channel-bed, a substantial amount of reflected energy can be produced. Moreover, in this figure one feature that is common to all the curves is the oscillating nature of the absolute values of the first-order coefficients as a function of *Ph*. It is also observed that reflected energy generated in this case is comparatively smaller than those of the upper surface is bounded by a free surface.

In Fig. 4, the first-order reflection coefficient $|R_1|$ is plotted against porosity parameters *Ph* for different number of ripples in the patch of the bottom deformation on the porous bed. For all curves, we consider the ripple wave number *lh* as l. It is clear from this figure that as the total number of ripples in the patch of the deformation on the porous bed $(m+n)/2$ increases, the value of p_0h converges to a number in the neighborhood of *lh*/2 and also the peak value of the reflection coefficient $|R_1|$ increases. But when the number of ripples, becomes very large, the reflection coefficient become unbounded. That means the perturbation expansion, which is discussed in section (3), ceases to be valid when the reflection coefficient becomes much larger than the deformation parameter, as pointed out by Mei (1985). Its oscillatory nature against *Ph* is more noticeable with the number of zeros of $|R_1|$ increased, but the general feature of $|R_1|$ remains the same.

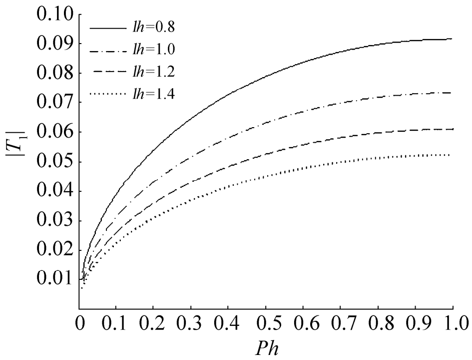

Fig.5 Variation of T_1 plotted for various ripple wave numbers of sinusoidal bed

Fig. 5, shows the non-dimensionalized first-order transmission coefficient $|T_1|$ against porosity parameters *Ph* of the channel-bed for different ripple wavenumbers $lh = 0.8, 1, 1.2$ and 1.4 in the patch of the deformation on the porous bed. In this figure, for all curves, we consider $m=2$ and $n=3$. Here also, it has been observed from this figure that as the ripple wavenumbers increase, the transmission coefficient $|T_1|$ becomes smaller than those for the smaller ripple wavenumbers. That means when an incident wave propagates over a porous channel-bed having a small ripple wavenumber in the patch of the deformation, a substantial amount of transmitted energy can be produced. From this figure, it is also clear that the non-oscillating nature of first-order correction to the transmitted energy $|T_1|$ as functions of the porosity parameters *Ph* of the channel-bed.

Furthermore, in this section, we have also checked the validation of the numerical values of reflection and transmission coefficients by showing the energy balance relation (52) is satisfied.

Consider an incident surface wave propagates over bottom deformation on a porous channel-bed. We have presented the variation of reflected energy $|R|$, transmitted energy $|T|$ and the energy balance relation $|R|^2+|T|^2$ for various values of porosity parameter in the following tables.

Table 1 Numerical values of $p_0h, |R|, |T|$ and $|R|^2+|T|^2$ for various values of *Ph* (exponentially damped deformation)

Ph	p_0h	$\lvert R\rvert$	$\lvert T\rvert$	$\lvert R\rvert^2+\lvert T\rvert^2$
0.01	0.100 166 97	0.002 347 80	1.000 005 54	1.000 016 59
0.21	0.474 927 91	0.001 978 32	1.000 107 70	1.000 219 32
0.41	0.687 493 44	0.001 867 59	1.000 190 78	1.000 385 08
0.61	0.869 829 02	0.001 900 66	1.000 251 30	1.000 506 27
0.81	1.040 838 28	0.001 984 89	1.000 287 03	1.000 578 09
1.01	1.208 014 26	0.002 092 15	1.000 297 80	1.000 600 08

Table 2 Numerical values of $p_0h, |R|, |T|$ and $|R|^2+|T|^2$ for various values of *Ph* (sinusoidal bed)

Ph	p_0h	$\lvert R\rvert$	$\lvert T\rvert$	$\lvert R\rvert^2+\lvert T\rvert^2$
0.01	0.100 166 97	0.000 001 39	1.000 499 16	1.000 998 57
0.21	0.474 927 91	0.012 839 77	1.002 201 49	1.004 572 69
0.41	0.687 493 44	0.001 351 16	1.002 930 17	1.005 870 74
0.61	0.869 829 02	0.002 223 35	1.003 363 00	1.006 742 26
0.81	1.040 838 28	0.003 517 21	1.003 594 22	1.007 213 72
1.01	1.208 014 26	0.004 238 84	1.003 661 04	1.007 353 46

In Table 1, the numerical values for $p_0h, |R|, |T|$ and $|R|^2+|T|^2$ are given for an exponentially damped deformation profile on the porous bed. In this case, we fixed the height of the hump taken as $a_0/h=0.2$ and the non-dimensionalized parameter bh as 0.3. Here we are able to successfully achieve the satisfaction of the energy balance relation almost accurately. Similarly, in Table 2, the numerical values for $p_0h, |R|, |T|$ and $|R|^2+|T|^2$ are given for another type of an undulating bottom profile namely a patch of sinusoidal ripples. In this case, we fixed the phase angle of the deformation $\vartheta=0$, the ripple wavenumber lh as 1, the values of m and n are taken as 2 and 3, respectively, the amplitude of the sinusoidal ripples a/h as 0.1, and the non-dimensional number ε as 0.05. From the numerical values of the reflection and transmission coefficients, we are able to successfully achieve the satisfaction of the energy balance relation or energy identity almost accurately.

7 Conclusions

In this paper, within the framework of two-dimensional linear water wave theory, we have developed the solution of the water wave scattering problem involving a small deformation on the porous bed in a channel, where the upper surface is bounded above by an infinitely extent rigid horizontal surface and the channel is unbounded in the horizontal direction. In such a situation, there exists only one mode of time-harmonic waves which propagate on the porous surface. A simplified perturbation analysis is employed to reduce the governing BVP to a simpler BVP for the first-order correction of the potential function. The first-order potential and, hence, the reflection and transmission coefficients are obtained by the method based on Fourier transform as well as Green's integral theorem with the introduction of appropriate Green's function. Two special examples of bottom deformation: the exponentially damped deformation and the sinusoidal ripple bed, are considered to validate the results. For the particular example of a patch of sinusoidal ripples, the main result that follows is that, the resonant interaction between the bed and the surface waves is attained in the neighborhood of a singularity, when the ripples wavenumber of the bottom deformation become approximately twice the components of the incident field wavenumber along the positive x-direction. This singularity point varies with porous effect parameters of the channel-bed and the ripple wave numbers on the bottom surface. It is also observed that a very few ripples may be needed to produce a substantial amount of reflected energy so that the amplitude of the generated waves increases. Also the theory discussed in this paper is valid only for infinitesimal reflection and away from resonance. The results obtained here are expected to be qualitatively helpful in tackling the water wave scattering problems with bottom deformations on a porous channel-bed. The theory can be applied in order to solve problems related to underground pipe bridge.

Acknowledgement

The author wishes to thank Prof. Swaroop Nandan Bora, Indian Institute of Technology Guwahati, India for his valuable discussions and suggestions to carry out the preparation of the manuscript.

References

Chakrabarti A, 2000. On the solution of the problem of scattering of surface-water waves by the edge of an ice cover. *Proceedings of The Royal Society of London, Series A*, **456**, 1087-1099.

Chwang AT, 1983. A porous-wavemaker theory. *Journal of Fluid Mechanics*, **132**, 395-406.
DOI: https://doi.org/10.1017/S0022112083001676

Davies AG, 1982. The reflection of wave energy by undulations of the sea bed. *Dynamics of Atmosphere and Oceans*, **6**, 207-232.

Hur PS, Mizutani N, 2003. Numerical estimation of wave forces acting on a three-dimensional body on submerged breakwater. *Coastal Engineering*, **47**(3), 329-345.
DOI: http://dx.doi.org/10.1016/S0378-3839(02)00128-X

Jeng DS, 2001. Wave dispersion equation in a porous seabed. *Ocean Engineering*, **28**(12), 1585-1599.
DOI: http://dx.doi.org/10.1016/S0029-8018(00)00068-8

Linton CM, Chung H, 2003. Reflection and transmission at the ocean/sea-ice boundary. *Wave Motion*, **38**(1), 43-52.
DOI: 10.1016/S0165-2125(03)00003-9

Maiti P, Mandal BN, 2014. Water wave scattering by an elastic plate floating in an ocean with a porous bed. *Applied Ocean Research*, **47**, 73-84.
DOI: http://dx.doi.org/10.1016/j.apor.2014.03.006

Mandal BN, Basu U, 2004. Wave diffraction by a small elevation of the bottom of an ocean with an ice-cover. *Archive of Applied Mechanics*, **73**, 812-822.
DOI 10.1007/s00419-004-0332-y

Martha SC, Bora SN, 2007. Oblique water-wave scattering by small undulation on a porous sea-bed. *Applied Ocean Research*, **29(**1-2), 86-90.
DOI: http://dx.doi.org/10.1016/j.apor.2007.07.001

Mei CC, 1985. Resonant reflection of surface water waves by periodic sandbars. *Journal of Fluid Mechanics*, **152**, 315-335.
DOI: https://doi.org/10.1017/S0022112085000714

Mohapatra S, 2014. Scattering of surface waves by the edge of a small undulation on a porous bed in an ocean with ice-cover. *Journal of Marine Science and Application*, **13**(2), 167-172.
DOI: 10.1007/s11804-014-1241-2

Mohapatra S, 2015. Scattering of oblique surface waves by the edge of a small undulation on a porous ocean bed. *Journal of Marine Science and Application*, **14**(2), 156-162.
DOI: 10.1007/s11804-015-1298-6

Mohapatra S, 2016. The interaction of oblique flexural gravity waves with a small bottom deformation on a porous ocean-bed: Green's function approach. *Journal of Marine Science and Application*, **15**(2), 112-122.
DOI: 10.1007/s11804-016-1353-y

Porter R, Porter D, 2003. Scattered and free waves over periodic beds. *Journal of Fluid Mechanics*, **483**, 129-163.
DOI: https://doi.org/10.1017/S0022112003004208

Porter D, Porter R, 2004. Approximations to wave scattering by an ice sheet of variable thickness over undulating topography. *Journal of Fluid Mechanics*, **509**, 145-179.
DOI: https://doi.org/10.1017/S0022112004009267

Sahoo T, Chan AT, Chwang AT, 2000. Scattering of oblique surface waves by permeable barrierrs. *Journal of Waterway, Port and Coastal Ocean Engineering*, **126(**4), 196-205.
DOI: http://dx.doi.org/10.1061/(ASCE)0733-950X(2000)126:4(196)

Silva R, Salles P, Palacio A, 2002. Linear wave propagating over a rapidly varying finite porous bed. *Coastal Engineering*, **44**(3), 239-260.
DOI: http://dx.doi.org/10.1016/S0378-3839(01)00035-7

Tsai CP, Chen HB, Lee FC, 2006. Wave transformation over submerged permeable breakwater on porous bottom. *Ocean Engineering*, **33**(11-12), 1623-1643.
DOI: http://dx.doi.org/10.1016/j.oceaneng.2005.09.006

Wang CM, Meylan MH, 2002. The linear wave response of a floating thin plate on water of variable depth. *Applied Ocean Research*, **24**(3), 163-174.
DOI: http://dx.doi.org/10.1016/S0141-1187(02)00025-1

Zhu S, 2001. Water waves within a porous medium on an undulating bed. *Coastal Engineering*, **42**(1), 87-101.
DOI: http://dx.doi.org/10.1016/S0378-3839(00)00050-8